Journal Pre-proof

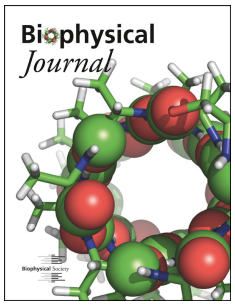

Methemoglobin formation in mutant Hemoglobin α-chains: electron transfer parameters and rates

Vaibhav A. Dixit, Jochen Blumberger, Shivam Kumar Vyas

PII: S0006-3495(21)00559-2

DOI: https://doi.org/10.1016/j.bpj.2021.07.007

Reference: BPJ 11205

To appear in: *Biophysical Journal*

Received Date: 28 April 2021

Accepted Date: 7 July 2021

Please cite this article as: Dixit VA, Blumberger J, Vyas SK, Methemoglobin formation in mutant Hemoglobin α-chains: electron transfer parameters and rates, *Biophysical Journal* (2021), doi: https://doi.org/10.1016/j.bpj.2021.07.007.

Methemoglobin formation in mutant Hemoglobin α-chains: electron transfer parameters and rates

Vaibhav A. Dixit,*[,a] Jochen Blumberger,[b] and Shivam Kumar Vyas[a]

[a] Department of Pharmacy, Birla Institute of Technology and Sciences Pilani (BITS-Pilani), Vidya Vihar Campus 41, Pilani, 333031, Rajasthan (India). E-mail: vaibhav.dixit@pilani.bits-pilani.ac.in, vaibhavadixit@gmail.com

[b] Department of Physics and Astronomy, University College London, Gower Street, London WC1E 6BT, U.K. Email: j.blumberger@ucl.ac.uk

A preliminary version of this work, https://doi.org/10.1101/2021.03.28.437393, was deposited in BioRxiv on 29/03/2021.

Abstract

Hemoglobin mediated transport of dioxygen (O_2) critically depends on the stability of the reduced (Fe^{2+}) form of the heme cofactors. Some protein mutations stabilize oxidized (Fe^{3+}) state (Methemoglobin, Hb M) causing methemoglobinemia and can be lethal above 30 %. Majority of the analyses of factors influencing Hb oxidation are retrospective and give insights only for inner sphere mutations of heme (His58, His87). Herein, we report the first all atom MD simulations on both redox states and calculations of the Marcus ET parameters for the α-chain Hb oxidation and reduction rates for Hb M. The Hb WT (wild type), and most of the studied α-chain variants maintain globin structure except the Hb M Iwate (H87Y). The mutants forming Hb M tend to have lower redox potentials and thus stabilize the oxidized (Fe^{3+}) state (in particular, the Hb Miyagi variant with K61E mutation). Solvent reorganization (λ_{solv} 73 – 96 %) makes major contributions to reorganization free energy, while protein reorganization (λ_{prot}) accounts for 27 – 30 % except for the Miyagi and J-Buda variants (λ_{prot} ~ 4 %). Analysis of heme-solvent H-bonding interactions among variants provide insights into the role of Lys61 residue in stabilizing the Fe^{2+} state. Semi-classical Marcus ET theory based calculations predict experimental k_{ET} for the Cyt b5:Hb complex and provides insights into relative reduction rates for Hb M in Hb variants. Thus our methodology provides a rationale for the effect of mutations on the structure, stability and Hb oxidation, reduction rates and has potential for identification of mutations that result in methemoglobinemia.

Significance

Hemoglobin function is dependent on the stability of the heme Ferrous (Fe^{2+}) state. Some mutants stabilize Ferric (Fe^{3+}) state leading to methemoglobin (Hb M) formation that can be fatal. Current literature provides only retrospective analysis for these findings. We utilized molecular dynamics (MD) simulations to calculate electron transfer (ET) parameters and provide biophysical insights into the mechanisms for Hb M formation and reduction. Further we modelled Hb:Cyt b5 complex dynamics and calculated ET parameters to estimate ET rates (k_{ET}) that agree closely with literature reports. Our methodology allows consistent prediction of ET parameters and reduction rates, which has potential use in the identification of mutations resulting in methemoglobinemia.

1. Introduction

Hemoglobin variants are wide spread in the Human population as seen in the HbVar database (http://globin.cse.psu.edu/hbvar/menu.html). These variants lead to two broad classes of disorders: 1) Globin synthesis and assembly disorders known as Thalassemias and 2) Globin structure disorders (Methemoglobinemia, Sickle cell anemia, and disorders caused by unstable, and altered dioxygen (O_2) affinity Hb variants).[1] Hb variant characterization, biochemical properties and associated clinical manifestations have been reviewed recently.[2,3] Hb is normally present in the reduced (Fe^{2+}, 99%) state and effectively transports O_2 between lungs and tissues. In red blood cells (RBCs), the concentration of the oxidized Hb, Methemoglobin (metHb, also known as Hb M), is kept below 1 % by enzymatic (NADPH dependent Flavin reductase, and Cytochrome b5) and non-enzymatic (e.g. ascorbic acid) reductive pathways.[4] Higher levels (~ 10 %) can lead to cyanosis, reduced O_2 delivery and level above 30 % can be lethal. This condition, known as Methemoglobinemia, can be induced by drugs (chloroquine/hydroxychloroquine), inherited defects in Cytochrome b5 (or its reductase), or inheritance of an Hb variant characterized by an increase in the stability of oxidized (Ferric, Fe^{3+}) or a decrease in the stability of the (ferrous, Fe^{2+}) states.[5–10] Methemoglobinemia has been reported in many COVID-19 patients,[11–13] thus potentially complicating the assessment of blood O_2 saturation levels in respiratory distress. Incidence of COVID-19 in patients with sickle cell disease (characterized by Hb S) was found to be 85 %, but prevalence of other Hb variants in COVID-19 patients remains unexplored.[14]

A large body of information and knowledge is available in the form of more than 1820 known variants, > 600 human Hb structures in the PDB, a large number of biochemical, genetic, spectroelectrochemical, and modeling studies. The structure and function of Hb and impact of mutations on O_2 affinity has been reviewed in the past.[15–17] The Hb globin structure has eight helices that maintain a hydrophobic environment around the heme and stabilize Fe^{2+} state to ensure reversible O_2 binding. Structural changes that destabilize the goblin or expose heme to solvent enhance oxidation rates and Hb M formation. Robust clinical and biochemical tests

(HPLC, Electrophoretic, MALDI-TOF and PCR), are available for the characterization of different variants, for example sickle cell Hb (Hb S), and thalassemic forms (Hb F),[3] but functional characterization of these variants in terms of O_2 affinity or Hb M content, oxidation, and reduction rates are extremely rare.[18]

Thus the in vivo rates for Hb oxidation to Hb M and reduction of Hb M back to Fe^{2+} state for many Hb variants remains unknown. These unknowns can potentially lead to failures in diagnosis, delays in the treatment, overtreatment and even cause treatment failures with standard therapy like methylene blue.[9,19] Additionally, due to the lack of knowledge of factors like optimum reductant concentrations, and O_2 pressures, Hb M content can go unrecognized and reach toxic levels causing cyanosis and even fatality. Thus reliable estimation of the relative Hb oxidation and Hb M reduction rates for different Hb variants is urgently required.

The experimental redox potentials ($E°$) for Hb and Hb subunits depend on the details of the experimental method (direct electrochemistry, or spectroelectrochemistry), nature of the electrodes and its interactions with Hb, and conditions e.g. presence of O_2, pH (Bohr effect), ionic strength, redox mediator, and temperature. Literature values range from -0.172 to + 0.050 V. In studies with the Hb tetramer, the identity of the subunits undergoing the redox changes are uncertain. Earlier Mateescu et al., have performed cyclic voltammetry experiments to determine the Hb $E°$s under acidic/aerobic and neutral/anaerobic conditions which are known to stabilize the T (tense) and R (relaxed) states respectively.[20] The authors assigned $E°$ values of -0.040 and -0.165 V respectively to the R and T states of Hb. Guiles et al, have measured the $E°$ of Hb, Cyt b5 and used Marcus theory to predict reorganization energies (λ) and homogenous and heterogenous ET rates.[21] Similar variations in the $E°$s were observed in the presence and absence of O_2 which are characteristic of R and T states.

Marcus theory of electron transfer (ET) and its variants have been successfully applied in the areas of material science, small molecule charge-transfer complexes, redox heme and non-heme proteins involved in respiratory and mitochondrial ET chains.[22] Since Hb is a tetramer with two identical α and β chains which contain identical Fe-porphyrin (heme) co-factor, experimental measurements of enzymatic and non-enzymatic Hb reduction rates for individual subunits and applications of ET theories has proved challenging. The generally accepted mechanism of Cyt b5 and Hb interaction is considered to involve an initial complex formation followed by the ET between the two proteins (Equation 1).[23,24] The observed rate constant, k_{app}, can be written as a product of the equilibrium constant of binding, k_b, and the rate constant for electron transfer, k_{ET}, $k_{app} = k_b * k_{ET}$. McLendon et al., have used reconstituted [Zn, Fe] hybrid Hb dimers in which heme Iron in one of the chains has been replaced with znic.[24] These hybrid Hbs show a larger free energy change (ΔG°) associated with the reduction (Equation 1) compared to the Hb wild type (WT). Due to the weaker interaction between Cyt b5 and Hb, these measurements were made at lower temperatures (~ 10 °C) and extrapolated to 25 °C.

Using Marcus theory and assuming a constant reorganization energy of (λ = 0.9 V) the authors calculated ET rates (k_{ET}) for the WT and hybrid Hb. The Hb WT k_{ET} = 1.6 s^{-1} was estimated to be in close agreement with experimental value of 1 and 2 s^{-1} at pH = 7 and 6 respectively at 10 °C. Based on the binding constant (k_b) and observed k_{app} = 770 M^{-1}, the authors calculated k_{ET} = 120 s^{-1} for the Hb WT at 25 °C. ET rates from the photoinduced excited state of hybrid Hb were about 1500 fold higher due to a larger driving force.

$$Cyt\ b5\ (Fe^{2+}) + Hb\ M\ (Fe^{3+}) \leftrightarrow\ Cyt\ b5\ (Fe^{2+})\ \ldots\ Hb\ M\ (Fe^{3+})$$
$$\rightarrow Cyt\ b5\ (Fe^{3+}) + Hb\ (Fe^{2+})$$

Equation 1

Earlier studies by Mauk et al., had found spectroscopic evidence for quantitative formation of 1:1 Cyt b5:Hb complexes.[25] Extending this work they proposed a model for the Cyt b5:Hb complex in which the heme edges are 8 Å apart while the Fe-Fe distance in the complex was 16 Å.[26] Hb residues (Lys 54, 56, 60, 61, 90, heme propionates) and Cyt b5 residues (Glu 43, 44, 48, Asp 60, and heme propionates) were postulated to be involved in complex formation. Later Hoffman et al., used similar Hb hybrids and determined the ET rates for individual Hb subunits.[27] The α subunit showed 4 fold higher binding affinity and 2 fold faster ET rates compared to the β subunits. These findings were similar to earlier reports of the ET between Hb and inorganic complexes.[28] Brittan et al., performed Brownian dynamics and electrostatics calculations to reassess the structural requirements for efficient electron transfer between Cyt b5 and embryonic Hb.[29] Although there was a descent agreement with Mauk et al,[25] regarding the identity of residues involved in the complex formation, the ET rates were overestimated for the Hb WT and were similar to the hybrid Hb. None of these studies have performed all atom MD simulations of the redox states to estimate Marcus parameters and ET rates.

A combination of quantum chemical calculations and MD simulations have been used to estimate Marcus ET parameters (λ, ΔG°) and ET rates for other redox proteins.[30–37] These methods make use of the linear response approximation to estimate the free energy parabolas which allows the estimation of λ, and ΔG° from the thermal averages of the energy gaps (<ΔE>) for the oxidized (O) and reduced (R) states.[32] ET rates can then be predicted using either the full estimation of electronic coupling matrix and Frank-Condon factors or using empirical parameters for protein packing density along with the Marcus parameters.[38,39] Studies with other redox proteins have shown that mutations both within and outside the active sites lead to significant changes in the Marcus parameters which ultimately modulate the ET rates and protein functions.[38,39,40,41] MD simulations for the Hb WT have been reported earlier.[42–48] These, mostly focused on the allosteric mechanisms of ligand binding and T → R transitions. More recently Case and Samuel have studied the dynamics of Hb M and associated heme loss.[49] But the calculations or estimations of the Marcus parameters and ET rates for Hb WT and its

variants using all atom MD simulations have not been reported to date and represent gaps in our understanding of how globin mutations influence Hb oxidation, reduction and Hb M content via modulation of ET parameters. Reliable predictions of ET parameters for Hb WT and its variants can provide atomic level and functional insights into factors influencing Hb oxidation. This information can prove valuable in identifying potential Hb variants with increased propensity for oxidation and Hb M formation. It may also prove useful in the design of novel alternative therapeutic interventions in populations where classical therapy (e.g. methylene blue) is contraindicated. Indeed the design of safer blood substitutes has been attempted, but clinical development has often been hampered by heme-oxidation induced toxicity.[50,51]

In this work, we performed all atom MD simulations on the Hb WT and variant α Hb chains and of the WT α Hb:Cyt b5 complex for the estimation of the parameters that determine the thermodynamics and kinetics of Hb reduction, in particular heme redox potentials ($E°$), driving force ($\Delta G°$), reorganization free energies (λ), electronic coupling (H_{ab}), ET activation free energies ($\Delta G^{‡}$) and ET rates (k_{ET}). We address the following key questions with respect to Hb oxidation and Hb M reduction among selected Hb variants. 1) What is the influence of Hb M stabilizing α chain mutations on the globin structure and stability? 2) Can a protocol utilizing quantum chemically derived parameters and all-atom MD simulations be used to estimate ET parameters for the α Hb chain and its redox partner Cyt b5? 3) What is the influence of Hb M stabilizing mutations on the ET parameters and ET rates? 4) How do these mutations affect outer-sphere (including protein and solvent) reorganization energies (namely, and $\lambda_{os} = \lambda_{prot} + \lambda_{solv}$) and the ET driving force? 5) Do these thermodynamic and kinetic parameters provide insights into the Hb M reduction rates? 6) Can the ET parameters and rates provide insights into the relative Hb M reduction rates among Hb variants?

2. Methodology

Protein preparation

Hemoglobin (Hb) α chain coordinates were extracted from T state structure 1HGA (A chain).[52,53] This structure represents the deoxy-Hb in the T state. As seen in Figure 1 alignment of the protein backbone of this structure with the oxidized methemoglobin (Hb M, 1HGB shows very similar structure (backbone and all atom RMSD = 0.186, 0.233 Å). Thus 1HGA structure was chosen for further analysis. The protonation states for the protein chain were estimated at pH = 7.4 with H++ 3.0[54] via its webserver.[55] Total charge on the globin chain was +1 at this pH. For Cyt b5 modeling, the 3NER[56] structure was selected and protein was prepared for MD simulations using a similar procedure. Total charge on the Cyt b5 structure was -11 at pH = 7.4. A TIP3P water box of 10 Å was added around the proteins, followed by counter ions (Na^{+}, or Cl^{-}) such that the proteins in the Fe^{2+} redox state are neutral and thus the Fe^{3+} states have +1 charge.

2.1. Heme parameterization with MCBP.py and quantum chemical calculations

Metal Center Bond Parameter python tool (MCBP.py)[57] available in AmberTools18[58] was used for heme and axial ligand parameterization in both the redox states of Cyt b5, Hb and Hb variants. A procedure similar to that described for the CYP450 BM3 (Amber advanced tutorial http://ambermd.org/tutorials/advanced/tutorial20/mcpbpy_heme.htm) was used (see Supplemental Information for details).

2.2. Equilibration and production simulations

A robust ten-step protocol recently reported by Roe and Brooks was used to equilibrate the structures of Hb α chains, its variants, Cyt b5 and Cyt b5:Hb complex studied in the present work.[59] Briefly, step 1 involved minimization of solvent while keeping strong (5.0 kcal/mol Å) restraints on the protein, porphyrin ring, Fe and the axial ligand. In Step 2, a short 15 ps MD with NVT, weak-coupling thermostat was performed while retaining the restraints. Step 3, was 1000 steps of minimization with weaker (2.0 kcal/mol Å) restraints on the same atom selection. Step 4, continued minimization for 1000 steps with even weaker (0.1 kcal/mol Å) restraints on the same atom selection. Step 5, final minimization for 1000 steps without any restraints. Step 6 was MD for 5 ps, with moderate (1.0 kcal/mol Å) restraints on the same atom selection using NPT ensemble. Step 7 and 8 were additional relaxation for 5 and 10 ps respectively with NPT and smaller (0.5 kcal/mol Å) restraints. Step 9, involved unrestrained relaxation for 10 ps. The final density equilibration was performed in 1 ns increments without any restraints under periodic boundary conditions, hydrogens were restrained with SHAKE on, a collision frequency was set to 5 ps^{-1} as recommended for Langevin thermostat and temperature was set to 300 K. This protocol defines three parameter values as a robust criteria for declaring the equilibration success. The criteria are 1) the value for the slope of the density vs. time plot should be less than 10^{-6}. 2) The final density of the system should not differ from the average of the second half of the density data by more than 0.02 g cm^{-3}. 3) The fitted exponential chi square value should be less than 0.5. All the structure simulated in the present work passed these criteria and thus were used for production runs and further analysis. This protocol available via AmberMDPrep shell script requires the latest version of cpptraj (V4.30.2) which was installed from GitHub and sourced before running the protocol.[60]

Figure 1. Alignment of α chains of hemoglobin structures in the reduced (1HGA, blue) and oxidized (1HGB, light orange) states. The Fe-N(HIS 87) distances in 1HGA and 1HGB are 2.214 and 2.153 Å respectively. The corresponding Fe-N(HIS 58) distances are 4.444 and 4.303 Å. These parameters are in agreement with the geometry of heme complexes where the Fe is displaced out of the plane of the porphyrin ring unless coordinated with additional axial ligands like O_2 and the oxidized state is low spin hexa coordinate usually interacts with water or with HIS 58. Dashed light yellow lines indicate that residues interact with each other. Amino acids in red-color indicate mutation sites studied in this work.

The structures for the Hb variants were prepared by renaming the chosen backbone residue names and deleting the sidechain atoms from the PDB file. The mutant side-chain rotamers without clashes and highest probability were selected from the Dunbrack's rotamer library

available in Chimera.[61,62] Identical protocols were used for equilibrating the Hb variant α chains in both redox (Fe^{2+} and Fe^{3+}) states. The summary of mutation categories in the Hbvar database contains information on 363 α chain variants. The summary table also gives 13 variants classified as Methemoglobins, 4 of which are α chain variants. Nonetheless, many of the 363 α chain variants (not classified in the database as Methemoglobins), do form Hb M. Thus we additionally selected variants which have been characterized in the literature[63] and are known to form methemoglobin (Hb M) and/or lower the concentration of reduced Hb namely, Hb M Boston (H58Y), Hb M Iwate (H87Y), Hb Miyagi (K61E) and Hb Kirklareli (H58L). Additionally, a single point mutant for which Hb M formation has not been reported, Hb J-Buda (K61N), was studied.

2.3. Protein-protein docking between Cyt b5 and Hb using HADDOCK webserver

Protein-protein docking between Cyt b5 (3NER) and Hb (1HGA) wild type (WT) α-chain was performed using HADDOCK 2.2. webserver.[64] The interacting residues mentioned in the introduction were chosen to dock the two proteins with no additional restraints. HADDOCK found 162 structures which were grouped into 7 clusters. As seen in Table S1, cluster 3 containing nine structures were found to have similar scores suggesting similar binding. A closer inspection of these HADDOCK predicted structures showed that the expected protein-protein and heme interactions were present in only the top ranked structure (HADDOCK score = -37.4 ± 6.0 and z-score = -1.1, see Figure 5). Furthermore, the cluster 3 showed most favorable Van der Waals, electrostatic energies and desolvation energy was comparable to other clusters. This prediction, where out of the many degenerate structures only a small fraction are ET competent (i.e. close heme-heme and favorable protein-protein interactions) is in agreement with the "Dynamic Docking" hypothesis proposed earlier by Wheeler et al., for the Cyt b5:Hb complex.[23] Thus this structure was prepared for MD simulations using the protein preparation, heme parameterization and equilibration protocol mentioned in section 2.1, and 2.2 above.

3. Results and Discussion

Reduction of the monomeric α chain of Hb WT has been studied earlier.[23,65] These studies found that the redox behavior of the α Hb chain in monomeric state is almost identical to the Hb tetramer. Thus studying the redox properties of a single α Hb monomer as done here is justified and can be expected to meaningfully represent the redox and ET processes in the tetramer. As noted by Hub et al., most of the experimental studies monitor the hydrogen bond dynamics between a small set of selected inter-chain residues e.g. αAsp94-βTrp37 and αTyr42-βAsp99.[44] These interactions are interpreted in terms of conformational transitions (T ↔ R) without further investigations. NMR studies in solution have identified α chain His45, Tyr42, Thr41, His89, His50, His72 residues play an important role in Bohr effect while residues around Asp94 and His122 participate in α1β2 subunit interactions.[17]

3.1. Influence of Hb α-chain mutations on the structure and stability

Realizing the dynamical nature of Hb α chain interactions the effect of Hb M stabilizing mutations on the dynamics and flexibility of various globin regions was investigated. Residue wise backbone root mean square fluctuations (RMSF) on the equilibrated trajectories (40 ns) were calculated with cpptraj (as seen in Figure 2). As expected the N and C-terminals show higher fluctuations. A comparison of the RMSF for residues ~10-130 shows that the overall globin structure is similar among variants except the Hb M Iwate which involves mutation of the axial Histidine ligand with Tyrosine (H87Y). This mutation is known to destabilize the heme globin structure and function.[66]

To assess the influence of other mutations which show a stable globin structure but nonetheless oxidize to Hb M, the RMSF values among their redox states were compared. For this a student T-test matrix among all the variants was calculated (See Table S2, Supplemental Information). Residue-wise RMS fluctuations (RMSF) are considered similar for pairs that show a P value more than 0.05. Mutation of the distal Histidine with Tyrosine (H58Y) seen with the Boston Hb variant maintains the overall globin structure. The largest backbone fluctuations are in the residues 44-54, 89, 90, and 114-119 (see Figure 2). The region 44-54 is a loop that has important hydrophobic (Phe43, 46-heme) and electrostatic (His45-heme carboxylate) interactions that stabilize the heme in the wild type. Whereas the region 114-119 has key interactions with the β chain residues (Arg30, and His116). The RMSF (excluding four terminal residues) for the redox state between WT and H58Y variant shows that fluctuations are significantly different and the average, min, max and stdev are larger for the H58Y variant (Table S2 and S3, see Supplemental Information). This indicates that this mutation destabilizes both the redox states.

Mutation of the His58 to Arg, analogous to the H58R Zurich variant of the β chain, shows similarly large variations in these regions in addition to a larger fluctuation in the loop 117-120. These findings are consistent with the large size of the Arg side chain (similar to Tyr) which leads to similar motions of these regions as manifested by higher RMSF value (see Figure 2). The fluctuations induced by H58R mutation are significantly different and average values are about twice from the Hb WT (Table S2 and S3).

Figure 2. RMSF for the protein backbone for the wild type Hb, mutants leading to the formation of Hb M (Iwate and Boston variants) and H58R mutant which is analogous to the β chain Hb Zurich variant. The RMSF was calculated for 2000 snapshots extracted from a 40 ns MD trajectory.

A close inspection of the globin and heme structure in Hb M Iwate during the MD simulation, shows that the heme group significantly moves out of the protein pocked and gets exposed to the solvent medium (see Figure S1). It is known in the literature that the Hb M Iwate structure is not stable and there is experimental evidence that the heme group gets transferred to the distal histidine in the reduced state.[66] Considering the large structural changes that H87Y

mutation induces in the Hb structure and the lack of crystal structure we choose not to use these MD trajectories to investigate the effect on Marcus parameters, oxidation energies and ET rates for this Hb variant.

The RMSF analysis for the Hb Miyagi and Kirklareli variants (K61E and H58L) which are known to form Hb M showed similar RMSF (pairwise) compared to the reduced (Fe^{2+}) and oxidized (Fe^{3+}) Hb WT. The average reduced (Fe^{2+}) RMSF is larger than the oxidized (Fe^{3+}) state for both these variants (Table S2 and S3). This is in contrast to the WT and other Hb variants suggesting that the reduced state fluctuations are higher in these variants. Recently a crystal structure (3QJD) for the Kirklareli variant has been reported.[67] Pairwise CA atom RMSD between the 1HGA and 3QJD is 1.00 Å, suggesting that the mutant adopts a similar globin structure (see Figure S3). MD simulations starting from this structure showed similar trends in RMSF. Nonetheless, the Fe^{2+} state showed larger fluctuations for polar residues Asn78, His89 and Lys90. This suggests that the His58 interactions with heme stabilize the movement of proximal residues and mutation to a non-polar Leucine thus increases the dynamics of these residues. The Fe^{3+} state, on the other hand, had higher RMSF in the loop region (residues 114-117). In contrast the Hb J-Buda variant with a semi-conservative mutation (K61N) showed minor fluctuations in the heme interacting loop (residues 44-54). Whereas relatively larger differences in fluctuations are observed in the region 115-120 which indicates weaker interactions with the β chain (especially in the oxidized state, see Figure 3). Except for the K61E, H58L variants, the RMSF values are consistently higher for the oxidized (Fe^{3+}) state. This can be understood by considering the reduction in the electrostatic repulsion between the Glu side-chain and the heme group in the oxidized state. These findings suggest that mutation in one region of the Hb can have significant influence on the dynamics in distant regions.[68,69]

Figure 3. Residue wise RMSF for the protein backbone for the Hb variants in the oxidized (Ferric) and reduced (Ferrous) states during the 40 ns MD simulations. The Hb Miyagi (K61E) and Hb Kirklareli variants forms Hb M, while the Hb J-Buda (K61N) variant functions normally.

A comparison of the RMSD between the Hb redox states for individual variants similarly shows that the variants leading to Hb M formation results in the largest movement in the protein backbone (see Supplemental Information Figures S4-S12).

3.2. Redox potentials ($E°$) and reorganization free energy (λ) for Hb WT, Hb mutants and Cyt b5.

The mutations studied in this work are within the Hb active site, additionally previous and present docking models of the Hb-Cyt b5 complex estimates the Fe-Fe distance between the two heme cofactors > 1 nm (or 10 Å).[70] Thus it is reasonable to expect that the Hb mutations studied here primarily affect the redox properties of the Hb heme. Hence we investigate whether there is a correlation between redox potentials and/or reorganization free energy for oxidation of Hb mutants and their propensity to form Hb M in experiments (Equation 2).

$$Redued\ Hb\ (R)\ \rightarrow Oxdized\ Hb\ (O) + e^{-}$$

Equation 2

The redox potentials of Hb WT and mutants are obtained using the linear response approximation, $E°_{abs} = (\langle \Delta E \rangle_R + \langle \Delta E \rangle_O)/(2e)$, where ΔE is the vertical energy gap, $\Delta E = E_O - E_R$, E_O and E_R the potential energies of the oxidized and reduced Hb (obtained from the AMBER force field energy[33]), $\langle \Delta E \rangle_M$, M = O, R denotes the average vertical energy gap, obtained along molecular dynamics trajectories run in oxidation state M, and e is the unit charge. In MD simulations in periodic boundary conditions the absolute (abs) vertical energy gaps are not related to experimental observables due to the arbitrary zero of the Ewald potential, but their relative differences are physically meaningful. Therefore, we calculate the relative redox potentials of the Hb mutants with respect to WT, $\Delta E° = E°_{abs}$(mutant)- $E°_{abs}$(WT) and add these shifts to the experimental redox potential of WT vs normal hydrogen electrode (NHE), $E°$(WT)= -0.165 V, to obtain our estimate for the redox potential of the mutants vs NHE, $E°$(mutant) = -0.165 V + $\Delta E°$. The reorganization free energy for oxidation is typically divided in an inner and outer sphere part, $\lambda = \lambda_{is} + \lambda_{os}$. Previous calculations have shown that the inner sphere contribution is very small for heme proteins (25 meV for a single bis-His coordinated heme) and is thus neglected[71] , $\lambda \sim \lambda_{os}$. The outer-sphere contribution is obtained from the linear response approximations, $\lambda_{os} = (\langle \Delta E_{os} \rangle_R - \langle \Delta E_{os} \rangle_O)/2$. Since non-polarizable force fields like the one used here are known to systematically overestimate outer-sphere reorganization free energies, the latter were scaled down uniformly by a factor of 1.6, as recommended in Ref.[32]

The results of the calculations are summarized in Table 1 and Table 2 (see also Table S4 and Table S5). We first discuss the α analogue of the Hb Zurich β variant where a distal Histidine is replaced by a non-coordinating Arginine residue (H58R). We find a significant increase in redox potential from -0.165 to +0.064 V. The increase is in accord with expectations in the sense that when a neutral residue in the active site is mutated into a positively charged residue the electron affinity of the cofactor increases. This indicates a lower equilibrium concentration of Hb M for this variant compared to WT. Although, this variant has not been reported in the literature yet, its β analogue, the Hb Zurich variant, has been found to be susceptible to oxidation (HbVar database). Our results suggest that this Hb (H58R) variant may not lead to a noticeable change in the background Hb M content. The situation is strikingly different for the

Hb Miyagi variant. In this mutant the active site residue Lys61 that forms a key H-bonding interactions with a heme carboxylate, is mutated into a Glu residue. This results in a large predicted decrease of redox potential from -0.165 to -0.296 V. This is in accord with expectations as the positively charged Lys is replaced by a negatively charge Glu. This suggests a higher equilibrium concentration of Hb M in agreement with experimental observations (HbVar database). The Hb J-Buda variant involves a mutation of the same Lys61 to a semi-conservative Asn residue. Going from a positively charged to a neutral residue, the decrease in redox potential is smaller, $E°$ = -0.204 V. Finally, the Hb Kirklareli variant involves the substitution of His58 with a Leucine. Our calculations predict a small decrease in the estimated $E°$ by only about 10 mV w.r.t. the WT. MD simulations starting from a more recently reported crystal structure for this variant (3QJD),[67] give a small increase in 15 mV w.r.t. WT. Neither simulation clearly support the experimental observation that Hb M content for this variant is markedly increased (HbVar database).[67]

Reorganization free energies of all mutants are very similar to the WT, the small changes amongst the mutants are insignificant in terms of ET rates, indicating that this parameter does not correlate with propensity for Hb M formation. The λ value for the WT (0.69 eV) is lower than the value reported by Blankman et al., for the Hb tetramer.[21] It should be noted that this value for the Hb tetramer include λ contributions from the β subunit which is known to undergo larger structural changes upon ligand binding and hence a slightly larger λ for the tetrameric complex is expected (Figure 8a, 10 of reference [43]).

We have also estimated the reorganization free energy for oxidation of Cyt b5, the protein that donates an electron to Hb. This parameter is needed later (section 3.4, and 3.5) for estimation of ET rates. Only one crystal structure for only one human Cyt b5 has been reported (3NER).[56] Thus this structure was used for the calculations. Protein preparation, heme parameterization and MD simulations were performed using the protocol mention in section 2. The energy gaps for the Cyt b5 are considerably larger than those predicted for Hb and its variants (see Table S4). This is probably due to the smaller size and associated larger conformational change in the protein structure upon oxidation. The λ value for Cyt b5 is also larger than for Hb, λ = 0.93 eV after scaling. This estimate is larger than the electrochemically determined value (λ = 0.44 eV[21]). This can be expected since the electrochemical adsorption and protein complexation significantly stabilizes the protein dynamics in Cyt b5 in comparison to isolated solution state. The redox potential of Cyt b5, -0.212 V from experiment, is more negative than for Hb WT resulting in a driving force of -0.047 eV.

Table 1. Computed redox potentials (vs NHE) and reorganization free energies for Hb, selected α chain Hb variants and Cyt b5.

Protein	**Mutation**	**λ[a]** (eV)	***E°*** [a] (V)	**Hb M formation**

Hb	WT	0.69	-0.165[b]	< 1 %
α analogue of the Hb Zurich β variant	H58R	0.72	-0.064	NA[c]
Hb Miyagi	K61E	0.73	-0.296	Increased Hb M formation
Hb J-Buda	K61N	0.67	-0.204	NA[c]
Hb Kirklareli	H58L	0.70	-0.176	Increased Hb M formation
Hb Kirklareli (3QJD)	H58L	0.69	-0.150	
Cyt b5 (3NER)	Wild	0.93	-0.212	Not applicable

[a] See main text for details of calculations.
[b] Experimental redox potential vs NHE for T-state Hb, from Ref. [20]
[c] Information not available in the Hbvar database and literature.

3.3. Contributions of protein and solvent to the reorganization energies

As mentioned earlier, the total reorganization energy (λ) comprises of the inner-sphere and outer-sphere contributions. Similar to cytochromes, the relatively rigid nature of the heme cofactor, causes the inner-sphere reorganization energies to be small for Hb and variants with mutations in the outer-sphere protein environment.[72] Table 2 shows the scaled protein reorganization energies (λ_{prot}), calculated by stripping the solvent and ions from MD trajectories and re-estimating the AMBER energies with ff19SB force filed. The solvent reorganization energies (λ_{solv}) are then estimated as the difference between the total and protein reorganization energies (i.e. $\lambda_{solv} = (\lambda - \lambda_{prot})$). For all the Hb variants including the wild type, the major contribution to total λ comes from the solvent reorganization (λ_{solv}: 0.514 to 0.706 eV, 73-97 %). For the Hb WT, the solvent contributes 76%. Nonetheless, the λ_{prot} are non-negligible for the Hb WT (0.162 eV, 24 %) and the Hb M Boston variant (0.179 eV, 25 %). The H58L (Hb Kirklareli) variant showed a larger protein reorganization (λ_{prot} = 0.186 eV, 27 %) and solvent reorganization (λ_{solv} = 0.514 eV, 73 %) comparable to the Hb WT in response to oxidation.

Table 2. Decomposition of outer-sphere reorganization free energy in protein and solvent contribution, all values in eV.

Hb α chain Variants	**Mutation**	**λ**	**λ_{prot}**	**λ_{solv}**	**% contribution of λ_{solv} to λ**
Hb	Wild	0.69	0.16	0.53	76
Hb M Boston	H58Y	0.69	0.17	0.52	75

α analogue of the Hb Zurich β variant	H58R	0.72	0.18	0.54	75
Hb Miyagi	K61E	0.73	0.02	0.71	97
Hb J-Buda	K61N	0.67	0.03	0.64	95
Hb Kirklareli	H58L	0.70	0.19	0.51	73

The Boston and H58R variants shows λ_{solv}, and λ_{prot} values similar to the Hb WT. In the Hb WT, the sidechain of Lys61 forms an average of two H-bonding interactions with the bulk water and one H-bond with heme carboxylates (see *Figure 4*). These H-bond interactions between residue 61 and heme are lost in the K61E Hb Miyagi variant. The glutamate residue in the K61E Hb variant now forms an average of 5.8 and 4.3 H-bonds with the bulk water molecules in the reduced (Fe^{2+}) and oxidized (Fe^{3+}) states respectively. The repulsion between the glutamate and heme carboxylate leads to a significant reorganization of solvent structure (λ_{solv} = 0.706 eV, 97 %) forced by increased H-bonding with the surrounding water molecules. The Lys61 residue of the wild type Hb forms H-bonds with the heme in 26 % of the frames and thus stabilizes the additional negative charge in the reduced (Fe^{2+}) state (0.07 % of the frames in oxidized, Fe^{3+} state). This reduces to negligible (0.0075 % of the frames) in the K61N variant and zero in the K61E variant. This explains the unexpectedly lower protein reorganization in these variants in response to oxidation. This suggests that the Lys61 residue play a key role in determining the protein reorganization in response to oxidation and mutation at this site (especially into a negatively charged amino acid) increases Hb M formation. The larger protein reorganization (λ_{prot}) in the Hb WT prevents faster oxidation to Hb M, but mutation of Lys to uncharged or negatively charged residues lowers the λ_{prot} facilitating Hb M formation. Although there is a corresponding increase in the λ_{solv}, this is likely to be spread out among the a large number of bulk water molecules thus keeping the activation free energy lower than the Hb WT.

The Hb J-Buda variant which involves a semi-conservative mutation (K61N) forms an average only 1.1 H-bond interactions with the bulk water (not shown), and no interactions with the heme group. This explains lowest average RMSF calculated for both the K61E and K61N variants (Table S3). Nonetheless, there is a difference of 0.068 eV in λ_{solv} between these two variants with the K61N (Hb J-Buda) being similar to the Hb WT. This coupled with the larger oxidation free energy difference (0.13 eV) for the Hb Miyagi (K61E) variant also offers logical explanation for its lower redox potential.

Figure 4. Number of H-bonds formed between the side chain of the residue 61, solvent water and heme carboxylate in the Hb WT (K61) and in the Hb M Miyagi variant (K61E) during the 40 ns MD simulation.

3.4 Modelling the Cyt b5:Hb WT complex

Since the early docking and Brownian dynamics attempts to model the Cyt b5:Hb complex, the explicit modeling of the complex and electron transfer (ET) parameters for the reduction of Hb by Cyt b5 has not received much attention.[23,26,29] Although the docking based models serve as

the starting point in the absence of complex crystal structures, some features like the heme edge-to-edge distances predicted by these models have been questioned earlier.[24] Thus protein-protein docking between Cyt b5 and Hb was followed by all atom explicit MD simulations to address these aspects. The bis-His heme of Cyt b5 was parameterized using the MCBP.py tool and a procedure similar to that given in section 2.1.

MD simulations for 40 ns in each of the redox states, namely Hb (Fe^{3+})-Cyt b5(Fe^{2+}) and Hb (Fe^{2+})-Cyt b5(Fe^{3+}), were performed. The docked complex with Cyt b5 in the reduced (R) and Hb in the oxidized (O) state showed Fe-Fe and a minimum heme edge-to-edge distances of 16.9 and 4.5 Å respectively (see Figure 5). The heme groups gradually move away from each other during the MD simulation giving an average value of 23.506 Å and 12.119 Å for the Fe-Fe and heme edge-to-edge distances respectively. An analysis of the intermolecular H-bonding interactions between the two proteins during the MD (Table S6 and S7) showed that Hb residues His89, Lys90, Arg92, Arg141 are the major H-bond donors, while Cyt b5 residues Glu191, Glu195, Gly209, Asp207 and heme carboxylates are the major H-bond acceptors. On the other hand, the Cyt b5 residues act as H-bond donor and Hb residues as H-bond acceptor only rarely (< 10 %). The analysis of native contacts between the two protein chains (Table S8) shows a similar interaction profile. These complementary interactions observed during MD simulations are different from those estimated from protein-protein docking simulations. This suggests that the protein complex is considerably dynamic and does not bind in one particularly stable conformation but samples different configurations. These observations are in agreement with the dynamic docking hypothesis.[23]

Using the Marcus formalism and linear response approximation the electron transfer (ET) between the two proteins can be modelled as shown in Equation 3, Equation 4, and Equation 5.

$$Cyt\ b5_{Red} + Hb_{oxd}\ (RO) \rightarrow Cyt\ b5_{oxd} + Hb_{Red}\ (OR)$$

Equation 3

The barrier for the ET can be estimated using Equation 4.

$$\Delta G^{\ddagger} = \left(\frac{(\lambda + \Delta G^{o})^2}{4\,\lambda}\right)$$

Equation 4

The ET rate can then be predicted using semi-classical Marcus theory and associated Equation 5. Where H_{ab} is the electronic coupling between the two heme cofactors, $\hbar$ is the modified Plank's constant, k_B is the Boltzmann constant, T = 300 K. ET parameters for the complex are shown in Table 3.

$$k_{ET} = \frac{2\pi}{\hbar} * |H_{ab}|^2 * (4\pi\lambda k_B T)^{-1/2} * e^{\left(\frac{-(\lambda + \Delta G^{\circ})^2}{4\lambda k_B T}\right)}$$

Equation 5

The electronic coupling (H_{ab}) can be estimated from its empirical distance dependence relationship (Figure 2 of reference [73]). Thus $H_{ab} = A * \exp[-\beta * (R - R_0)/2]$, where the pre-exponential factor is 0.022 eV, β = 1.39 Å^{-1}, R_0 = 3.6, R is the heme edge-to-edge distance between the proteins. Using the average of the minimum heme edge-to-edge distance (12.1 Å) from the MD simulation gives a small coupling energy, $H_{ab} = 5.9 * 10^{-5}$ eV. The reorganization free energy for ET is estimated as the sum of the reorganization free energy of the isolated proteins (corresponding to ET at infinite ET distance) and effect of finite ET distance (12.1 Å) was accounted for using the Marcus continuum formula for outer-sphere reorganization. All ET parameters are summarized in Table 3. This gives an estimate of k_{ET} = 185.8 s^{-1} for the ET, in close agreement with the ~ 120 s^{-1} reported by Qiao et al.,[24] for the reaction at 25 °C. Our predictions are also higher than the electrochemical rate measurements (k_{ET} = 0.037 s^{-1}) reported by Blankman et al.,[21] who used the work term and electrostatics corrections on the predictions from Marcus and Sutin's relationship between ET kinetics and electrode half reactions.[74] This disagreement between electrochemical and solution ET values is expected since ET at the electrodes is known to be usually slower than in native protein complexes. Using Equation 4 the ET barrier ($\Delta G^{\ddagger}$) for the wild type complex was calculated to be 0.323 eV. Considering the experimental uncertainty of about 0.1 eV (2.3 kcal/mol) this can be considered as a reasonable agreement with experimental value of 4 kcal/mol value reported by Simons et al.[24] Thus we use the same procedure to calculate the ET rates from Cyt b5 to Hb variants in the next section.

Figure 5. Shortest heme edge-to-edge and Fe-Fe distances (Å) in the Cyt b5:Hb complex. A) Show these distances in the initial structure and B) show the evolution of these distances during a 40 ns MD simulation.

3.5 Rates for ET between Cyt b5 and Hb α-chain variants

To assess the influence of mutation we focused on the prediction of relative changes in the ET rates (k_{ET}) and barriers ($\Delta G^{\ddagger}$) for the reduction of Hb variants using Marcus ET parameters calculated in sections 3.2. Since these variants involve single point mutations of residues within the Hb active site with close interactions with heme, it is reasonable to assume that they have little impact on the protein-protein interactions in Cyt b5 and Hb complexes and thus the electronic coupling ($H_{ab} = 5.9 * 10^{-5}$ eV) remains small. Thus the ET λ for the Hb variants can be considered equal to the sum of the ET λ for the wild type complex and difference of oxidation λ between the mutant and the Hb WT α-chain (Table 3). Thus, for example, using values in Table 1 and Table 3, the ET λ for the H58R Hb variant complex with Cyt b5 is 1.420 = (1.384 + (0.721 - 0.6853). The ET free energy change ($\Delta G°$) is equal to the difference in the redox potentials ($\Delta E°$) between the Cyt b5 and the Hb variant.

Thus ET barriers ($\Delta G^{\ddagger}$) and rates (k_{ET}) for Cyt b5:Hb variant complexes can be calculated using Equation 4 and Equation 5 respectively and are shown in Table 3. Our predictions for the ET rate suggest that the Hb M of the H58R variant will be reduced faster upon oxidization to Hb M. The ET rate for the Hb Miyagi variant is lowest at 9.1 s^{-1}. Hence, this variant not only features the highest equilibrium concentration of Hb M but also the slowest Hb M reduction rates. ET rate

and $\Delta G^{\ddagger}$ calculations for the J-Buda variant suggests that this variant will be reduced slower than the Hb WT. Additionally, the lower *E*° predicted for this variant also suggests that the equilibrium concentration of Hb M for the J-Buda variant might be higher than the Hb WT. Thus the presence of this variant should be assessed carefully in the patient groups at higher risk of oxidative stress.

For the Hb Kirklareli variant the ET rate (k_{ET} = 242.5 and 130.9 s^{-1}) calculated using the 3QJD and 1HGA structures respectively give an average similar to the Hb WT. The ET barrier ($\Delta G^{\ddagger}$) is also calculated to be similar to the wild type. Nonetheless, the lower *E*° estimated for this variant suggests higher equilibrium Hb M concentration that is in agreement with in vitro experimental findings and clinical reports.

Table 3. Parameters and rates for ET from Cyt b5 to Hb M WT and variants.

Protein	Mutation	ΔG° (eV)	λ (eV)	$\Delta G^{\ddagger}$ (eV)	k_{ET} (s^{-1})
Hb	WT	-0.047[a]	1.384	0.323	185.8 (exp. 120)[24]
α analogue of the Hb Zurich β variant	H58R	-0.148	1.420	0.285	797.7
Hb Miyagi	K61E	0.084	1.428	0.401	9.1
Hb J-Buda	K61N	-0.008	1.368	0.338	104.9
Hb Kirklareli (3QJD)	H58L	-0.047	1.385	0.323	242.5

[a] Experimental driving force for ET from Cyt b5 to Hb.

Conclusions

In summary, the answer to the questions asked in the introduction are as follows. 1) The single point mutations studied here, mostly do not disrupt the globin structure. Major exceptions to this are the His → Tyr mutations (Hb M Boston; distal site and Hb M Iwate, proximal). In the latter variant a heme transfer to Tyr is reported in the literature. Mutants K61E, K61N, H58R and H58L show influence on the selected regions of the globin chain (loop 44-54 and region 114-120). 2) All atom MD simulations and average vertical energy gap calculations allow reasonably accurate prediction of Marcus parameters (λ, ΔG°) that are in agreement with literature reports on similar heme proteins. 3) All the Hb M forming mutations (H58Y, K61E and H58L) lead to a marginal increase in the total reorganization energy (λ) associated with the Hb oxidation. Whereas the Hb J-Buda (K61N) shows a small decrease in λ. The calculated redox potentials are in correspondence with the known propensity of these variants to form Hb M. 4) The solvent reorganization (λ_{solv}) makes the largest contributions for all the variants (including the Hb WT). The mutation of the Lys residue has the largest influence on the protein reorganization energies (λ_{prot}) thus highlighting its role in the stabilization of the reduced (Fe^{2+})

state, normal Hb structure and function. 5) The calculated Marcus ET parameters, redox potentials offer explanation for the corresponding higher and moderate propensity of Hb oxidation to Hb M for the K61E and K61N mutants respectively. Our calculations are also consistent with the reports that H58L variant (Hb Kirklareli) undergoes faster autoxidation (lower $E°$ than Hb WT). 6) Calculations of the ET parameters and reduction rate predictions using MD simulations for the Cyt b5:Hb complex and semi-classical Marcus ET theory are in close agreement with experimental measurements. Additionally, reduction rate prediction of Hb variants are also in agreement with available in vitro rate data and clinical observations of Hb M formation. Thus a combination of thermodynamic ($E°$) and kinetic ($\Delta G^{‡}$, k_{ET}) considerations allows us to rationalize formation of Hb M in Miyagi, Kirklareli variants and lack thereof in the Hb WT and J-Buda.

Finally, this study represents the first attempt to calculate Marcus parameters for the oxidation of Hb and reduction rates of Hb M using all atom MD simulations of the redox states. Our GPU enabled MD simulations, post-processing, calculations and data analysis completes within 4-5 hour/mutant. Thus this methodology can be applied to other Hb variants and heme proteins to extract meaningful predictions and may have a potential to guide experimental studies on most medically relevant, and industrially useful mutations.

Funding information

This work is partially supported by funding from Additional Competitive Research Grant (ACRG) BITS Pilani (PLN/AD/2019-20/13).

Author contributions

VAD conceptualized the project, wrote funding proposal, performed literature search, calculations, analyzed results, wrote the manuscript and participated in discussions. JB analyzed the results, provided expert opinion, participated in manuscript writing and discussions. SKV performed preliminary literature and database search, and participated in discussions.

References

(1) Forget, B. G.; Franklin Bunn, H. Classification of the Disorders of Hemoglobin. *Cold Spring Harb. Perspect. Med.* **2013**, *3* (2). https://doi.org/10.1101/cshperspect.a011684.

(2) Thom, C. S.; Dickson, C. F.; Gell, D. A.; Weiss, M. J. Hemoglobin Variants: Biochemical Properties and Clinical Correlates. *Cold Spring Harb. Perspect. Med.* **2013**, *3* (3). https://doi.org/10.1101/cshperspect.a011858.

(3) Wajcman, H.; Moradkhani, K. Abnormal Haemoglobins: Detection & Characterization. *Indian Journal of Medical Research*. Wolters Kluwer -- Medknow Publications October 2011, pp 538–546.

(4) Kinoshita, A.; Nakayama, Y.; Kitayama, T.; Tomita, M. Simulation Study of

Methemoglobin Reduction in Erythrocytes. *FEBS J.* **2007**, *274* (6), 1449–1458. https://doi.org/10.1111/j.1742-4658.2007.05685.x.

(5) Toker, I.; Yesilaras, M.; Tur, F. C.; Toktas, R. Methemoglobinemia Caused by Dapsone Overdose: Which Treatment Is Best? *Turkish J. Emerg. Med.* **2015**, *15* (4), 182–184. https://doi.org/10.1016/j.tjem.2014.09.002.

(6) McRobb, C. M.; Holt, D. W. Methylene Blue-Induced Methemoglobinemia during Cardiopulmonary Bypass? A Case Report and Literature Review. *J. Extra. Corpor. Technol.* **2008**, *40* (3), 206–214.

(7) Bilgin, H.; Özcan, B.; Bilgin, T. Methemoglobinemia Induced by Methylene Blue Pertubation during Laparoscopy. *Acta Anaesthesiol. Scand.* **1998**, *42* (5), 594–595. https://doi.org/10.1111/j.1399-6576.1998.tb05173.x.

(8) Rosen, P. J.; Johnson, C.; McGehee, W. G.; Beutler, E. Failure of Methylene Blue Treatment in Toxic Methemoglobinemia. Association with Glucose-6-Phosphate Dehydrogenase Deficiency. *Ann. Intern. Med.* **1971**, *75* (1), 83–86. https://doi.org/10.7326/0003-4819-75-1-83.

(9) Patnaik, S.; Natarajan, M. M.; James, E. J.; Ebenezer, K. Methylene Blue Unresponsive Methemoglobinemia. *Indian J. Crit. Care Med.* **2014**, *18* (4), 253–255. https://doi.org/10.4103/0972-5229.130582.

(10) Jaffey, J. A.; Harmon, M. R.; Villani, N. A.; Creighton, E. K.; Johnson, G. S.; Giger, U.; Dodam, J. R. Long-Term Treatment with Methylene Blue in a Dog with Hereditary Methemoglobinemia Caused by Cytochrome B5 Reductase Deficiency. *J. Vet. Intern. Med.* **2017**, *31* (6), 1860–1865. https://doi.org/10.1111/jvim.14843.

(11) Lopes, D. V.; Lazar Neto, F.; Marques, L. C.; Lima, R. B. O.; Brandão, A. A. G. S. Methemoglobinemia and Hemolytic Anemia after COVID-19 Infection without Identifiable Eliciting Drug: A Case-Report. *IDCases* **2021**, *23*, e01013. https://doi.org/10.1016/j.idcr.2020.e01013.

(12) Scholkmann, F.; Restin, T.; Ferrari, M.; Quaresima, V. The Role of Methemoglobin and Carboxyhemoglobin in COVID-19: A Review. *J. Clin. Med.* **2020**, *10* (1), 50. https://doi.org/10.3390/jcm10010050.

(13) Naymagon, L.; Berwick, S.; Kessler, A.; Lancman, G.; Gidwani, U.; Troy, K. The Emergence of Methemoglobinemia amidst the COVID-19 Pandemic. *American Journal of Hematology*. Wiley-Liss Inc. August 1, 2020, pp E196–E197. https://doi.org/10.1002/ajh.25868.

(14) Menapace, L. A.; Thein, S. L. COVID-19 and Sickle Cell Disease. *Haematologica*. Ferrata Storti Foundation November 1, 2020, pp 2501–2504. https://doi.org/10.3324/haematol.2020.255398.

(15) Ahmed, M. H.; Ghatge, M. S.; Safo, M. K. Hemoglobin: Structure, Function and Allostery. In *Subcellular Biochemistry*; Springer, 2020; Vol. 94, pp 345–382.

https://doi.org/10.1007/978-3-030-41769-7_14.

(16) Marengo-Rowe, A. J. Structure-Function Relations of Human Hemoglobins. *Baylor Univ. Med. Cent. Proc.* **2006**, *19* (3), 239–245. https://doi.org/10.1080/08998280.2006.11928171.

(17) Lukin, J. A.; Ho, C. The Structure-Function Relationship of Hemoglobin in Solution at Atomic Resolution. *Chem. Rev.* **2004**, *104* (3), 1219–1230. https://doi.org/10.1021/cr940325w.

(18) Yudin, J.; Verhovsek, M. How We Diagnose and Manage Altered Oxygen Affinity Hemoglobin Variants. *Am. J. Hematol.* **2019**, *94* (5), 597–603. https://doi.org/10.1002/ajh.25425.

(19) Khanal, R.; Karmacharya, P.; Pathak, R.; Poudel, D. R.; Ghimire, S.; Alweis, R. Do All Patients with Acquired Methemoglobinemia Need Treatment? A Lesson Learnt. *J. Community Hosp. Intern. Med. Perspect.* **2015**, *5* (5), 29079. https://doi.org/10.3402/jchimp.v5.29079.

(20) Ciureanu, M.; Goldstein, S.; Mateescu, M. A. Direct Electron Transfer for Hemoglobin in Surfactant Films Cast on Carbon Electrodes. *J. Electrochem. Soc.* **1998**, *145* (2), 533–541. https://doi.org/10.1149/1.1838299.

(21) Blankman, J. I.; Shahzad, N.; Miller, C. J.; Guiles, R. D. Direct Voltammetric Investigation of the Electrochemical Properties of Human Hemoglobin: Relevance to Physiological Redox Chemistry. *Biochemistry* **2000**, *39* (48), 14806–14812. https://doi.org/10.1021/bi000731b.

(22) Ritter, S. Five Decades Of Marcus Theories. *Chem. Eng. News* **2006**, *84* (42).

(23) Wheeler, K. E.; Nocek, J. M.; Cull, D. A.; Yatsunyk, L. A.; Rosenzweig, A. C.; Hoffman, B. M. Dynamic Docking of Cytochrome B5 with Myoglobin and α-Hemoglobin: Heme-Neutralization "Squares" and the Binding of Electron-Transfer-Reactive Configurations. *J. Am. Chem. Soc.* **2007**, *129* (13), 3906–3917. https://doi.org/10.1021/ja067598g.

(24) Qiao, T.; Simmons, J.; Horn, D. A.; Chandler, R.; McLendon, G. Electron Transfer from Cytochrome B5 to Methemoglobin. *J. Phys. Chem.* **1993**, *97* (50), 13089–13091. https://doi.org/10.1021/j100152a010.

(25) Mauk, M. R.; Mauk, A. G. Interaction between Cytochrome B5 and Human Methemoglobin. *Biochemistry* **1982**, *21* (19), 4730–4734. https://doi.org/10.1021/bi00262a032.

(26) Poulos, T. L.; Mauk, A. G. Models for the Complexes Formed between Cytochrome B5 and the Subunits of Methemoglobin. *J. Biol. Chem.* **1983**, *258* (12), 7369–7373. https://doi.org/10.1016/S0021-9258(18)32188-4.

(27) Naito, N. R.; Huang, H.; Sturgess, A. W.; Nocek, J. M.; Hoffman, B. M. Binding and Electron Transfer between Cytochrome B5 and the Hemoglobin α- and β-Subunits

through the Use of [Zn, Fe] Hybrids. *J. Am. Chem. Soc.* **1998**, *120* (44), 11256–11262. https://doi.org/10.1021/ja982009v.

(28) Eguchi, L. A.; Saltman, P. Kinetics and Mechanisms of Metal Reduction by Hemoglobin. 2. Reduction of Copper(II) Complexes. *Inorg. Chem.* **1987**, *26* (22), 3669–3672. https://doi.org/10.1021/ic00269a011.

(29) Kidd, R. D.; Baker, E. N.; Brittain, T. A Modeling Study of the Interaction and Electron Transfer between Cytochrome B5 and Some Oxidized Haemoglobins. *J. Biol. Inorg. Chem.* **2002**, *7* (1–2), 23–30. https://doi.org/10.1007/s007750100261.

(30) Hu, L.; Farrokhnia, M.; Heimdal, J.; Shleev, S.; Rulíšek, L.; Ryde, U. Reorganization Energy for Internal Electron Transfer in Multicopper Oxidases. *J. Phys. Chem. B* **2011**, *115* (45), 13111–13126. https://doi.org/10.1021/jp205897z.

(31) Tipmanee, V.; Oberhofer, H.; Park, M.; Kim, K. S.; Blumberger, J. Prediction of Reorganization Free Energies for Biological Electron Transfer: A Comparative Study of Ru-Modified Cytochromes and a 4-Helix Bundle Protein. *J. Am. Chem. Soc.* **2010**, *132* (47), 17032–17040. https://doi.org/10.1021/ja107876p.

(32) Blumberger, J. Recent Advances in the Theory and Molecular Simulation of Biological Electron Transfer Reactions. *Chemical Reviews*. American Chemical Society 2015, pp 11191–11238. https://doi.org/10.1021/acs.chemrev.5b00298.

(33) Blumberger, J. Free Energies for Biological Electron Transfer from QM/MM Calculation: Method, Application and Critical Assessment. *Phys. Chem. Chem. Phys.* **2008**, *10* (37), 5651–5667. https://doi.org/10.1039/b807444e.

(34) Krishtalik, L. I. The Medium Reorganization Energy for the Charge Transfer Reactions in Proteins. *Biochim. Biophys. Acta - Bioenerg.* **2011**, *1807* (11), 1444–1456. https://doi.org/10.1016/j.bbabio.2011.07.002.

(35) Kaila, V. R. I.; Johansson, M. P.; Sundholm, D.; Wikström, M. Interheme Electron Tunneling in Cytochrome c Oxidase. *Proc. Natl. Acad. Sci. U. S. A.* **2010**, *107* (50), 21470–21475. https://doi.org/10.1073/pnas.1005889107.

(36) Jiang, X.; Futera, Z.; Ali, M. E.; Gajdos, F.; Von Rudorff, G. F.; Carof, A.; Breuer, M.; Blumberger, J. Cysteine Linkages Accelerate Electron Flow through Tetra-Heme Protein STC. *J. Am. Chem. Soc.* **2017**, *139* (48), 17237–17240. https://doi.org/10.1021/jacs.7b08831.

(37) Jiang, X.; Van Wonderen, J. H.; Butt, J. N.; Edwards, M. J.; Clarke, T. A.; Blumberger, J. Which Multi-Heme Protein Complex Transfers Electrons More Efficiently? Comparing MtrCAB from Shewanella with OmcS from Geobacter. *J. Phys. Chem. Lett.* **2020**, *11*, 9421–9425. https://doi.org/10.1021/acs.jpclett.0c02842.

(38) Hosseinzadeh, P.; Lu, Y. Design and Fine-Tuning Redox Potentials of Metalloproteins Involved in Electron Transfer in Bioenergetics. *Biochim. Biophys. Acta - Bioenerg.* **2016**, *1857* (5), 557–581. https://doi.org/10.1016/j.bbabio.2015.08.006.

(39) Page, C. C.; Moser, C. C.; Chen, X.; Dutton, P. L. Natural Engineering Principles of Electron Tunnelling in Biological Oxidation-Reduction. *Nature* **1999**, *402* (6757), 47–52. https://doi.org/10.1038/46972.

(40) Alvarez-Paggi, D.; Castro, M. A.; Tórtora, V.; Castro, L.; Radi, R.; Murgida, D. H. Electrostatically Driven Second-Sphere Ligand Switch between High and Low Reorganization Energy Forms of Native Cytochrome C. *J. Am. Chem. Soc.* **2013**, *135* (11), 4389–4397. https://doi.org/10.1021/ja311786b.

(41) DiCarlo, C. M.; Vitello, L. B.; Erman, J. E. Effect of Active Site and Surface Mutations on the Reduction Potential of Yeast Cytochrome c Peroxidase and Spectroscopic Properties of the Oxidized and Reduced Enzyme. *J. Inorg. Biochem.* **2007**, *101* (4), 603–613. https://doi.org/10.1016/j.jinorgbio.2006.12.006.

(42) Saito, M.; Okazaki, I. A 45-Ns Molecular Dynamics Simulation of Hemoglobin in Water by Vectorizing and Parallelizing COSMOS90 on the Earth Simulator: Dynamics of Tertiary and Quaternary Structures. *J. Comput. Chem.* **2007**, *28* (6), 1129–1136. https://doi.org/10.1002/jcc.20640.

(43) Yusuff, O. K.; Babalola, J. O.; Bussi, G.; Raugei, S. Role of the Subunit Interactions in the Conformational Transitions in Adult Human Hemoglobin: An Explicit Solvent Molecular Dynamics Study. *J. Phys. Chem. B* **2012**, *116* (36), 11004–11009. https://doi.org/10.1021/jp3022908.

(44) Hub, J. S.; Kubitzki, M. B.; de Groot, B. L. Spontaneous Quaternary and Tertiary T-R Transitions of Human Hemoglobin in Molecular Dynamics Simulation. *PLoS Comput. Biol.* **2010**, *6* (5), e1000774. https://doi.org/10.1371/journal.pcbi.1000774.

(45) Fischer, S.; Olsen, K. W.; Nam, K.; Karplus, M. Unsuspected Pathway of the Allosteric Transition in Hemoglobin. *Proc. Natl. Acad. Sci. U. S. A.* **2011**, *108* (14), 5608–5613. https://doi.org/10.1073/pnas.1011995108.

(46) Laberge, M.; Yonetani, T. Molecular Dynamics Simulations of Hemoglobin a in Different States and Bound to DPG: Effector-Linked Perturbation of Tertiary Conformations and HbA Concerted Dynamics. *Biophys. J.* **2008**, *94* (7), 2737–2751. https://doi.org/10.1529/biophysj.107.114942.

(47) Yonetani, T.; Laberge, M. Protein Dynamics Explain the Allosteric Behaviors of Hemoglobin. *Biochimica et Biophysica Acta - Proteins and Proteomics*. Elsevier September 1, 2008, pp 1146–1158. https://doi.org/10.1016/j.bbapap.2008.04.025.

(48) Mouawad, L.; Perahia, D.; Robert, C. H.; Guilbert, C. New Insights into the Allosteric Mechanism of Human Hemoglobin from Molecular Dynamics Simulations. *Biophys. J.* **2002**, *82* (6), 3224–3245. https://doi.org/10.1016/S0006-3495(02)75665-8.

(49) Samuel, P. P.; Case, D. A. Atomistic Simulations of Heme Dissociation Pathways in Human Methemoglobins Reveal Hidden Intermediates. *Biochemistry* **2020**, *59* (42), 4093–4107. https://doi.org/10.1021/acs.biochem.0c00607.

(50) Cooper, C. E.; Silkstone, G. G. A.; Simons, M.; Rajagopal, B.; Syrett, N.; Shaik, T.; Gretton, S.; Welbourn, E.; Bülow, L.; Eriksson, N. L.; et al. Engineering Tyrosine Residues into Hemoglobin Enhances Heme Reduction, Decreases Oxidative Stress and Increases Vascular Retention of a Hemoglobin Based Blood Substitute. *Free Radic. Biol. Med.* **2019**, *134*, 106–118. https://doi.org/10.1016/j.freeradbiomed.2018.12.030.

(51) Silkstone, G. G. A.; Silkstone, R. S.; Wilson, M. T.; Simons, M.; Bülow, L.; Kallberg, K.; Ratanasopa, K.; Ronda, L.; Mozzarelli, A.; Reeder, B. J.; et al. Engineering Tyrosine Electron Transfer Pathways Decreases Oxidative Toxicity in Hemoglobin: Implications for Blood Substitute Design. *Biochem. J.* **2016**, *473* (19), 3371–3383. https://doi.org/10.1042/BCJ20160243.

(52) Liddington, R.; Derewenda, Z.; Dodson, E.; Hubbard, R.; Dodson, G. High Resolution Crystal Structures and Comparisons of T-State Deoxyhaemoglobin and Two Liganded T-State Haemoglobins: T(α-Oxy)Haemoglobin and T(Met)Haemoglobin. *J. Mol. Biol.* **1992**, *228* (2), 551–579. https://doi.org/10.1016/0022-2836(92)90842-8.

(53) RCSB PDB - 1HGB: HIGH RESOLUTION CRYSTAL STRUCTURES AND COMPARISONS OF T STATE DEOXYHAEMOGLOBIN AND TWO LIGANDED T-STATE HAEMOGLOBINS: T(ALPHA-OXY)HAEMOGLOBIN AND T(MET)HAEMOGLOBIN https://www.rcsb.org/structure/1hgb (accessed Jan 4, 2021).

(54) Anandakrishnan, R.; Aguilar, B.; Onufriev, A. V. H++ 3.0: Automating PK Prediction and the Preparation of Biomolecular Structures for Atomistic Molecular Modeling and Simulations. *Nucleic Acids Res.* **2012**, *40* (W1), W537–W541. https://doi.org/10.1093/nar/gks375.

(55) H++ (web-based computational prediction of protonation states and pK of ionizable groups in macromolecules) http://biophysics.cs.vt.edu/ (accessed Jan 5, 2021).

(56) Parthasarathy, S.; Altuve, A.; Terzyan, S.; Zhang, X.; Kuczera, K.; Rivera, M.; Benson, D. R. Accommodating a Nonconservative Internal Mutation by Water-Mediated Hydrogen Bonding between ß-Sheet Strands: A Comparison of Human and Rat Type B (Mitochondrial) Cytochrome b 5. *Biochemistry* **2011**, *50* (24), 5544–5554. https://doi.org/10.1021/bi2004729.

(57) Li, P.; Merz, K. M. MCPB.Py: A Python Based Metal Center Parameter Builder. *J. Chem. Inf. Model.* **2016**, *56* (4), 599–604. https://doi.org/10.1021/acs.jcim.5b00674.

(58) Case, D. A.; Ben-Shalom, I. Y.; Brozell, S. R.; Cerutti, D. S.; Cheatham, III, T. E.; Cruzeiro, V. W. D.; Darden, T. A.; Duke, R. E.; Ghoreishi, D.; Gilson, M. K.; et al. AMBER18. University of California: San Francisco 2018.

(59) Roe, D. R.; Brooks, B. R. A Protocol for Preparing Explicitly Solvated Systems for Stable Molecular Dynamics Simulations. *J. Chem. Phys.* **2020**, *153* (5), 054123. https://doi.org/10.1063/5.0013849.

(60) Roe, D. R.; Cheatham, T. E. PTRAJ and CPPTRAJ: Software for Processing and Analysis of

Molecular Dynamics Trajectory Data. *J. Chem. Theory Comput.* **2013**, *9* (7), 3084–3095. https://doi.org/10.1021/ct400341p.

(61) Shapovalov, M. V.; Dunbrack, R. L. A Smoothed Backbone-Dependent Rotamer Library for Proteins Derived from Adaptive Kernel Density Estimates and Regressions. *Structure* **2011**, *19* (6), 844–858. https://doi.org/10.1016/j.str.2011.03.019.

(62) Pettersen, E. F.; Goddard, T. D.; Huang, C. C.; Couch, G. S.; Greenblatt, D. M.; Meng, E. C.; Ferrin, T. E. UCSF Chimera - A Visualization System for Exploratory Research and Analysis. *J. Comput. Chem.* **2004**, *25* (13), 1605–1612. https://doi.org/10.1002/jcc.20084.

(63) Sussner, H.; Mayer, A.; Brunner, H.; Fasold, H. Raman Study on the Two Quaternary States of Unligated Hemoglobin. *Eur. J. Biochem.* **1974**, *41* (3), 465–469. https://doi.org/10.1111/j.1432-1033.1974.tb03288.x.

(64) Van Zundert, G. C. P.; Rodrigues, J. P. G. L. M.; Trellet, M.; Schmitz, C.; Kastritis, P. L.; Karaca, E.; Melquiond, A. S. J.; Van Dijk, M.; De Vries, S. J.; Bonvin, A. M. J. J. The HADDOCK2.2 Web Server: User-Friendly Integrative Modeling of Biomolecular Complexes. *J. Mol. Biol.* **2016**, *428* (4), 720–725. https://doi.org/10.1016/j.jmb.2015.09.014.

(65) Naito, N. R.; Hui, H. L.; Noble, R. W.; Hoffman, B. M. Determination of the Hemoglobin Surface Domains That React with Cytochrome B5. *Biochemistry* **2001**, *40* (7), 2060–2065. https://doi.org/10.1021/bi0021028.

(66) Jin, Y.; Nagai, M.; Nagai, Y.; Nagatomo, S.; Kitagawa, T. Heme Structures of Five Variants of Hemoglobin M Probed by Resonance Raman Spectroscopy. *Biochemistry* **2004**, *43* (26), 8517–8527. https://doi.org/10.1021/bi036170g.

(67) Bissé, E.; Schaeffer-Reiss, C.; Van Dorsselaer, A.; Alayi, T. D.; Epting, T.; Winkler, K.; Benitez Cardenas, A. S.; Soman, J.; Birukou, I.; Samuel, P. P.; et al. Hemoglobin Kirklareli (α H58L), a New Variant Associated with Iron Deficiency and Increased CO Binding. *J. Biol. Chem.* **2017**, *292* (6), 2542–2555. https://doi.org/10.1074/jbc.M116.764274.

(68) Tyukhtenko, S.; Rajarshi, G.; Karageorgos, I.; Zvonok, N.; Gallagher, E. S.; Huang, H.; Vemuri, K.; Hudgens, J. W.; Ma, X.; Nasr, M. L.; et al. Effects of Distal Mutations on the Structure, Dynamics and Catalysis of Human Monoacylglycerol Lipase. *Sci. Rep.* **2018**, *8* (1), 1–17. https://doi.org/10.1038/s41598-017-19135-7.

(69) Kang, S. A.; Crane, B. R. Effects of Interface Mutations on Association Modes and Electron-Transfer Rates between Proteins. *Proc. Natl. Acad. Sci. U. S. A.* **2005**, *102* (43), 15465–15470. https://doi.org/10.1073/pnas.0505176102.

(70) Simmons, J.; McLendon, G.; Qiao, T. Electron Transfer and Energy Transfer in the Hb:Hb Reductase (Cyt B5) System. *J. Am. Chem. Soc.* **1993**, *115* (11), 4889–4890. https://doi.org/10.1021/ja00064a059.

(71) Breuer, M.; Zarzycki, P.; Shi, L.; Clarke, T. A.; Edwards, M. J.; Butt, J. N.; Richardson, D. J.; Fredrickson, J. K.; Zachara, J. M.; Blumberger, J.; et al. Molecular Structure and Free

Energy Landscape for Electron Transport in the Decahaem Cytochrome MtrF. In *Biochemical Society Transactions*; Portland Press, 2012; Vol. 40, pp 1198–1203. https://doi.org/10.1042/BST20120139.

(72) Sigfridsson, E.; Olsson, M. H. M.; Ryde, U. A Comparison of the Inner-Sphere Reorganization Energies of Cytochromes, Iron-Sulfur Clusters, and Blue Copper Proteins. *J. Phys. Chem. B* **2001**, *105* (23), 5546–5552. https://doi.org/10.1021/jp0037403.

(73) Jiang, X.; Burger, B.; Gajdos, F.; Bortolotti, C.; Futera, Z.; Breuer, M.; Blumberger, J. Kinetics of Trifurcated Electron Flow in the Decaheme Bacterial Proteins MtrC and MtrF. *Proc. Natl. Acad. Sci. U. S. A.* **2019**, *116* (9), 3425–3430. https://doi.org/10.1073/pnas.1818003116.

(74) Marcus, R. A.; Sutin, N. Electron Transfers in Chemistry and Biology. *BBA Reviews On Bioenergetics*. Elsevier August 1, 1985, pp 265–322. https://doi.org/10.1016/0304-4173(85)90014-X.